SUBJECT-CENTERED MULTI-VIEW FEATURE FUSION FOR NEUROIMAGING RETRIEVAL AND CLASSIFICATION

Sidong Liu[⋆†]*, Weidong Cai* [⋆†]*, Siqi Liu*[⋆]*, Sonia Pujol*[†]*, Ron Kikinis*[†]*, Dagan Feng*[⋆‡]

[⋆] BMIT Research Group, School of IT, University of Sydney, Sydney, Australia
[†] Surgical Planning Lab, Brigham & Women's Hospital, Harvard Medical School, Boston, USA
[‡] Med-X Research Institute, Shanghai Jiaotong University, Shanghai, China

ABSTRACT

Multi-View neuroimaging retrieval and classification play an important role in computer-aided-diagnosis of brain disorders, as multi-view features could provide more insights of the disease pathology and potentially lead to more accurate diagnosis than single-view features. The large inter-feature and inter-subject variations make the multi-view neuroimaging analysis a challenging task. Many multi-view or multi-modal feature fusion methods have been proposed to reduce the impact of inter-feature variations in neuroimaging data. However, there is not much in-depth work focusing on the inter-subject variations. In this study, we propose a subject-centered multi-view feature fusion method for neuroimaging retrieval and classification based on the propagation graph fusion (PGF) algorithm. Two main advantages of the proposed method are: 1) it evaluates the query online and adaptively reshapes the connections between subjects according to the query; 2) it measures the affinity of the query to the subjects using the subject-centered affinity matrices, which can be easily combined and efficiently solved. Evaluated using a public accessible neuroimaging database, our algorithm outperforms the state-of-the-art methods in retrieval and achieves comparable performance in classification.

Index Terms— multi-view, neuroimaging, retrieval, classification

1. INTRODUCTION

Neuroimaging plays an important role in computer-aided-diagnosis of neurological disorders, such as Alzheimers disease (AD), Frontotemporal dementia (FTD), and Mild Cognitive Impairment (MCI). Most of the previous neuroimaging studies focus on the analysis of the disease-specific features extracted from the imaging data. Many single-view features, such as the brain grey matter volume [1], the cortical surface gyrification [2], the cortical folding pattern [3], the curvature [4], and the surface area [5], have been extensively studied. Recent research on multi-view/multi-modal neuroimaging analysis suggests that the complementary neuropathological insights in multi-view/multi-modal data could lead to better analysis results [6, 7]. However, the large inter-feature and inter-subject variations in the multi-view features make the complementary information extraction challenging.

With increasing attention given in the multi-view analysis, a number of multi-view feature fusion methods have been proposed. A straightforward solution is to concatenate input multi-view features into a high-dimensional vector, and then apply dimension reduction or feature selection methods, such as t-test [8], ISOMAP [9], Elastic Net [10, 11], or the combination of these methods [12, 13], to reduce the 'curse of dimensionality'. These methods show promising results. However, the inter-subject variations cannot be eliminated using the concatenation-based methods because the inter-subject distances measured by different features may have different scales and variations.

Recently, the multi-view analysis advances rapidly due to the research efforts on the multi-view embedding (ME) and the multi-kernel (MK) methods. ME methods, such as Multi-View Spectral Embedding (MSE) [14, 15] and Multi-View Local Linear Embedding (MLLE) [16], are based on the manifold-learning and could explore the geometric structures of local patches in multiple feature spaces and align the local patches in a unified feature space with maximum preservation of the geometric relationships. MK methods, such as the MK-Support Vector Machine (MK-SVM) [6] and the Multifold Bayesian Kernelization (MBK) [7], are fundamentally different from ME methods. They construct a set of kernels that can maximize the performance in single-view feature spaces, and then combine the kernelized features. Although ME and MK methods could reduce the inter-feature variations, the unpredictable variations among the unseen queries pose a bottleneck on the performance.

In this study, we propose a subject-centered multi-view feature fusion method for neuroimaging retrieval and classification based on the Propagation Graph Fusion (PGF) algorithm [17], which could adaptively reshape the connections between the subjects according to query, thus to find more relevant subjects. We conduct two experiments to validate

This work was supported in part by the ARC, AADRF , NA-MIC (U54 EB005149), and NAC (P41 EB015902).

the proposed method based on a publicly accessible database, Alzheimer's Disease Neuroimaging Initiatives (ADNI), with 758 magnetic resonance (MR) images. Our method shows a modest improvement over the state-of-the-art multi-view methods in retrieval, and also achieves comparable performance in classification.

2. METHODS

2.1. Neuroimaging Database and Multi-View Features

The neuroimaging data used in this work were obtained from the Alzheimer's Disease Neuroimaging Initiative (ADNI) [18]. Totally 758 T1-weighted MR volumes were selected from the baseline ADNI database, including 180 AD patients, 374 MCI patients and 204 cognitively normal (CN) elderly. All of these MR volumes were examined and corrected according the ADNI image correction protocols [18]. We registered the images to the ICBM-152 template [19] using the Image Registration Toolkit (IRTK) [20], and then parcellated them into 83 functional regions of interest (ROI) using the multi-atlas propagation with the enhanced registration approach (MAPER) [21]. From each MR volume, we extracted 6 types of widely used features to describe patients from different perspectives, including the grey matter volume [1] for capturing the size variations of cortical regions, the local gyrification index [2] for quantifying the cortical surface gyrification, the curvedness and shape index [3] for extracting the cortical folding patterns, and the convexity and the solidity [7] for measuring the effects of brain atrophy. All these features were localized features extracted from the 83 brain functional ROIs for each subject.

2.2. Subject-Centered Affinity Matrix Construction

The distances between two images in different feature spaces reflect their geometric relationships in different views. To preserve the local geometric structures, we construct a neighborhood for each subject in each feature space. Assuming N_v views of features have been extracted from N_d images in the database $\mathbb{D}$ and denoting x_i an image in the database and X the feature set, the neighborhood of x_i in the n^{th} feature space is formed by itself and its k nearest neighbors, i.e., $X_i^{(n)} = x_i^{(n)}, x_{i_1}^{(n)}, \ldots, x_{i_k}^{(n)}$. We establish the connections between the subjects by measuring the consistency of their neighborhoods using the Jaccard coefficient as in Eq.(1):

$$w(x_i^{(n)}, x_j^{(n)}) = \frac{|X_i^{(n)} \cap X_j^{(n)}|}{|X_i^{(n)} \cup X_j^{(n)}|} \tag{1}$$

These connections form the directed paths linking the subjects to each other. When a query x_q comes, we apply the same procedure to construct its neighborhood $X_q^{(n)}$ and determine its relative position in the feature space. Then we use the position of the query as the origin, and let x_q walk the paths to its k nearest neighbors $x_{q_1}^{(n)}, \ldots, x_{q_k}^{(n)}$. The query continues to propagate its walk from $x_{q_1}^{(n)}, \ldots, x_{q_k}^{(n)}$ to their nearest neighbors in $X_{q_1}^{(n)}, \ldots, X_{q_k}^{(n)}$ in the next iteration. The propagation stops until there is no other neighbor to be found. The longer it takes for the query to reach a subject, the less relevant that subject is expected to be. Thus, the links between subjects reflect the affinity of the query and the subjects. Taking into account this damping effect, we update the connection weights with regard to a specific query as in Eq.(2):

$$w'(x_i^{(n)}, x_j^{(n)}) = \alpha^{t_q(x_i^{(n)}, x_j^{(n)})} \cdot w(x_i^{(n)}, x_j^{(n)}) \tag{2}$$

where α is a weight decay parameter to control the damping effect of the walk and $t_q(x_i^{(n)}, x_j^{(n)})$ is the number of itera-

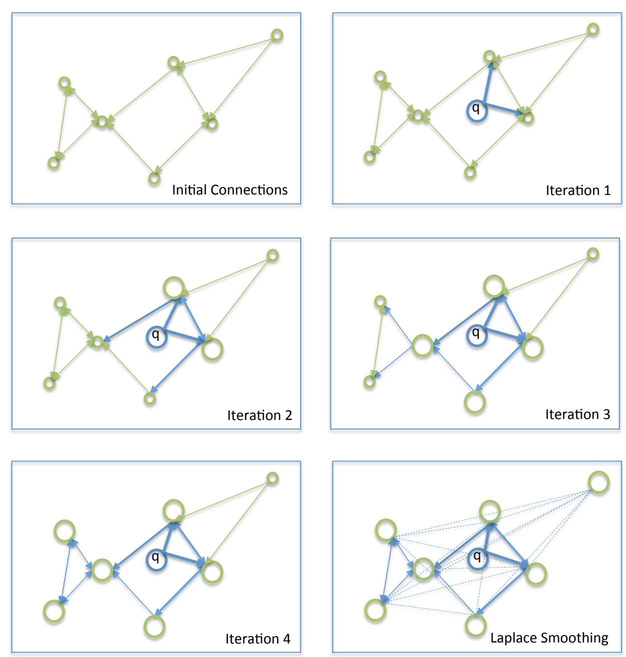

Fig. 1: A toy example of the subject-centered affinity matrix construction. The connections between the subjects, based on 2 nearest neighbors, could form directed paths, as indicated by the green lines. The query at the center, as indicated by the blue circle, visits its nearest neighbors in the first iteration and then propagates to other neighbors alone the paths in following iterations. The large green circles represent the subjects that have been visited by the query, and the blue lines show the routes. In this example, the propagation stops after 4 iterations. However, there is still one subject unvisited and some edges not weighted. We then perform the Laplace smoothing to add a weak weight to all the edges, as indicated by the dashed blue lines.

tions to reach the link $(x_i^{(n)}, x_j^{(n)})$. If a link is visited multiple times, we select the smallest t_q for it.

The updated weights are saved in a $N_d \times N_d$ affinity matrix, A, as in Eq.(3):

$$A(i,j) = w'(x_i^{(n)}, x_j^{(n)}) \tag{3}$$

This affinity matrix can be very sparse because many edges might not be visited through the propagation. However, sparsity is not a desirable property in our algorithm, because it will reduce the coverage of the candidate relevant subjects when we fuse the affinity matrices using the geometric means (see details in Section 2.3). Therefore, we apply the Laplace smoothing to A by adding a small value of $1/N_d$ to all the elements in A. Finally, we normalize A to guarantee it is row-stochastic, i.e., each row sums to 1, as in Eq.(4):

$$A'(i,j) = \frac{A(i,j) + 1/N_d}{\sum_{X_j \in \mathbb{D}} A(i,l) + 1} \tag{4}$$

An example of the subject-centered affinity matrix construction is given in Fig. 1.

2.3. Affinity Matrix Fusion

For each query, a group of affinity matrices, $A^{(1)}, \ldots, A^{(N_v)}$, can be obtained. Instead of using the arithmetic mean as in PGF [17], we use the geometric mean to fuse the affinity matrices in this study to avoid the offset effect of the arithmetic mean, as in Eq.(5):

$$A^*(i,j) = \sqrt[N_v]{\Pi_{n=1}^{N_v} A^{(n)}(i,j)} \tag{5}$$

Fig. 2 demonstrates the multi-view fusion with the arithmetic mean and the geometric mean respectively. The database contains three subjects as marked by different shapes. Fig. 2a shows three views of the feature spaces as indicated by different colors. The similarity between the query and each subject is indicated by the concentric circles, where lower value indicates smaller similarity. Fig. 2b shows that it is not sufficient to differentiate the subjects using the arithmetic mean. However, as shown in Fig. 2c, the geometric mean tends to give highly reliable results compared to the arithmetic mean, for it measures the conformity of the retrieval results across multiple views.

Our method requires $A^{(n)}(i,j) \neq 0$, since otherwise the link $(x_i^{(n)}, x_j^{(n)})$ will be disconnected regardless of the connections in other feature spaces. This will block the paths for the query to access the potential relevant candidates. This problem is solved by Laplace smoothing during the affinity matrix construction as described in Section 2.2.

The weights in A^* reflect the overall connectivity between different subjects and their affinity to the query. If we take A^* as a transition matrix, an equilibrium state exists to reflect the probabilities of the subjects to be visited. The subjects can be re-ranked according to their probabilities. The PageRank algorithm is applied to derive the equilibrium distributions, same as in [23].

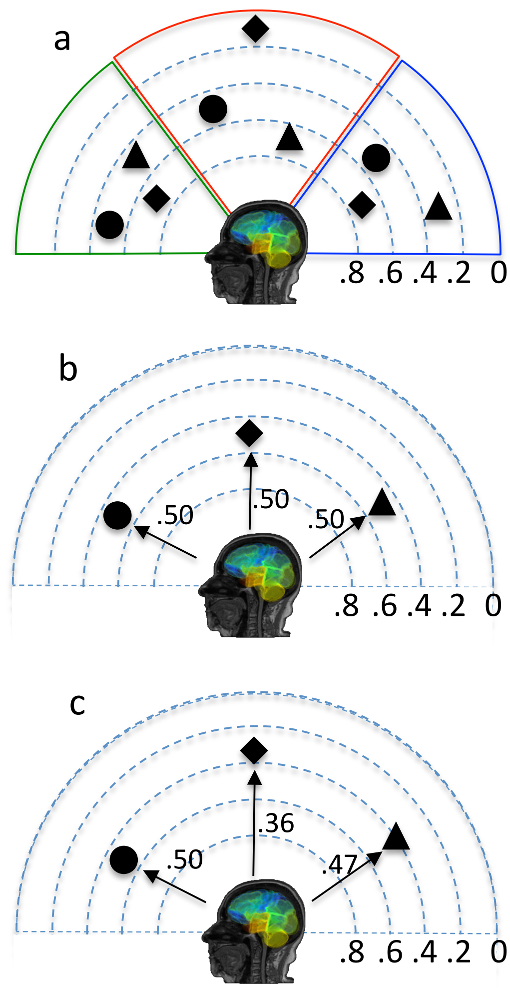

Fig. 2: The comparison of the results derived from arithmetic mean and geometric mean. The brain images are generated using 3D Slicer (V4.3) [22].

3. EXPERIMENTS AND RESULTS

Two experiments were conducted to validate our proposed method. Since PGF explores the connections between subjects and their affinity to the query, one natural application of PGF is the content-based image retrieval.

Another application of the PGF method is the multi-view classification. The equilibrium distributions derived from affinity matrix fusion are used as the feature representations in the experiment of classification.

Table 1: The performance of different retrieval methods

	CON	MSE	PGFa	PGFg
MAP(1)	60.8	62.6	67.0	70.4
MAP(3)	53.0	54.8	58.4	60.0
MAP(5)	49.6	51.3	54.1	55.0

Table 2: The CN vs. AD classification performance

	Accuracy	Sensitivity	Specificity
MK-SVM	76.5±0.9	80.2±1.5	72.2±1.0
PGFg-SVM	73.7±7.7	69.4±15.5	77.4±11.1

Table 3: The CN vs. MCI classification performance

	Accuracy	Sensitivity	Specificity
MK-SVM	65.6±1.0	37.5±2.1	80.9±1.1
PGFg-SVM	64.9±4.2	75.7±4.0	45.0±10.5

3.1. Experiment I: Unsupervised Multi-View Retrieval

The PGF with geometric mean (PGFg) was compared to the concatenation method (CON), MSE [14], and PGF with arithmetic mean (PGFa) [17]. We adopted the query-by-example paradigm and the leave-one-out cross-validation strategy for all the methods. The performance was evaluated using the Mean Average Precision (MAP) [12] with different cut-off numbers (1, 3, 5) of the relevant results. The number of nearest neighbors for constructing the local neighborhood was set as $k = 10$ for PGF and MSE. Other hyper-parameters for these methods were optimized through random search [24].

Table 1 shows performance comparison of different retrieval methods. The best single-view feature out of the 6 extracted features was the grey matter volume, with a MAP(1) of 61.1%. The CON method has the worst performance, since it suffers from the large feature variations. MSE shows better performance than the CON method, with slight improvements of 1.8% in MAP(1), 1.8% in MAP(3) and 1.7% in MAP(5). Larger improvements are achieved by PGFa and PGFg, which might benefit from the subject-centered workflows. PGFa had an improvement of 4.4%, 3.6% and 2.8% over MSE in MAP(1), MAP(3) and MAP(5), respectively. PGFg, benefited from the geometric mean, further improved PGFa by 3.4% in MAP(1), 1.6% in MAP(3) and 0.9% in MAP(5).

3.2. Experiment II: Supervised Multi-View Classification

Two classification tasks were conducted in this experiment, i.e., 1) classifying AD (positive) from CN (negative), and 2) classifying MCI (positive) from CN (negative). The equilibrium distributions derived by PGF were used to train the SVM classifier. Our PGFg-SVM method was compared to the MK-SVM method [6] based on 10-fold cross validation. Elastic Net [10] was applied to select the features for MK-SVM. The optimal hyper-parameters for both PGFg-SVM and MK-SVM were chosen by random search [24].

Overall, PGFg-SVM achieved comparable performance with MK-SVM in both tasks. The accuracy of PGFg-SVM was very close to that of MK-SVM. However, the sensitivity and specificity of these two algorithms were dramatically different, which suggested that MK-SVM and PGFg-SVM may have different strengths and potentially could enhance each other. MCI group usually has larger inter-subject variations than AD and CN groups, since MCI has overlaps with both AD and CN groups. MCI is the pre-symptomatic status of AD, and MCI patients have ongoing memory problems but not enough to interfere with daily activities. The sensitivity and specificity differences in task 1 and task 2 show that the proposed PGF-based algorithm is more robust to the large inter-subject variations, whereas the MK method could perform better when the inter-subject variations are small.

PGFg-SVM also had much greater standard deviations than MK-SVM, since PGF is a non-parametric method depending heavily on relationships between subjects. The classification performance of PGF might be restricted when the training set is not sufficient. However, it has potential to be extended when larger databases become available.

4. CONCLUSION

In this study, we proposed a subject-centered multi-view feature fusion method for neuroimaging retrieval and classification, which could evaluate the query online and adaptively reshape the connections between subjects for retrieving more relevant subjects. Compared to the conventional multi-view methods, our method could reduce the variations at both the feature and query levels and outperform the state-of-the-art methods in retrieval when evaluated on the same database. Our method also achieved comparable performance as the MK method in classification. Theoretically, our method is more robust to the large inter-subject variations compared to the MK method, but further investigation are needed to confirm this with additional experiments on larger datasets.

References

[1] Stefan Klöppel, Cynthia M. Stonnington, Carlton Chu, Bogdan Draganski, Rachael I. Scahill, Jonathan D. Rohrer, et al., "Automatic Classification of MR Scans in Alzheimer's Disease," *Brain*, vol. 131, no. 3, pp. 681 – 689, 2008.

[2] M. Schaer, M.B. Cuadra, L. Tamarit, F. Lazeyras, S. Eliez, and J. Thiran, "A Surface-Based Approach to Quantify Local Cortical Gyrification," *IEEE Transactions on Medical Imaging*, vol. 27, no. 2, pp. 161–170, 2008.

[3] David M. Cash, Andrew Melbourne, Marc Modat, M. Jorge Cardoso, et al., "Cortical Folding Analysis on Patients with Alzheimer's Disease and Mild Cognitive Impairment," in *Medical Image Computing and Computer-Assisted Intervention (MICCAI)*, vol. 7512 of *LNCS*, pp. 289–296. Springer Berlin Heidelberg, 2012.

[4] Suyash P. Awate, Paul A. Yushkevich, Zhuang Song, et al., "Cerebral Cortical Folding Analysis with Multivariate Modeling and Testing: Studies on Gender Differences and Neonatal Development," *NeuroImage*, vol. 53, no. 2, pp. 450–459, 2010.

[5] Sidong Liu, Weidong Cai, Yang Song, Sonia Pujol, et al., "Localized Sparse Code Gradient in Alzheimer's Disease Staging," in *Annual International Conference of the IEEE Engineering in Medicine and Biology Society (EMBC)*, pp. 5398–5401. 2013.

[6] Daoqiang Zhang, Yaping Wang, Luping Zhou, Hong Yuan, and Dinggang Shen, "Multimodal Classification of Alzheimer's Disease and Mild Cognitive Impairment," *NeuroImage*, vol. 55, no. 3, pp. 856 – 867, 2011.

[7] Sidong Liu, Yang Song, Weidong Cai, Sonia Pujol, et al., "Multifold Bayesian Kernelization in Alzheimer's Diagnosis," in *Medical Image Computing and Computer-Assisted Intervention (MICCAI)*, vol. 8150 of *LNCS*, pp. 303–310. Springer Berlin Heidelberg, 2013.

[8] Sidong Liu, Weidong Cai, Lingfeng Wen, Stefan Eberl, Michael J. Fulham, and Dagan Feng, "Generalized Regional Disorder-Sensitive-Weighting Scheme for 3D Neuroimaging Retrieval," in *Annual International Conference of the IEEE Engineering in Medicine and Biology Society (EMBC)*, pp. 7009–7012. 2011.

[9] Hyunjin Park, "ISOMAP Induced Manifold Embedding and Its Application to Alzheimer's Disease and Mild Cognitive Impairment," *Neuroscience Letters*, vol. 513, no. 2, pp. 141–145, 2012.

[10] Li Shen, Sungeun Kim, Yuan Qi, Mark Inlow, et al., "Identifying Neuroimaging and Proteomic Biomarkers for MCI and AD via the Elastic Net," in *Multimodal Brain Image Analysis (MBIA)*, vol. 7012 of *LNCS*, pp. 27–34. Springer Berlin Heidelberg, 2011.

[11] Si Qi Liu, Sidong Liu, Weidong Cai, Hangyu Che, et al., "Multi-Modal Neuroimaging Feature Learning for Multi-Class Diagnosis of Alzheimer's Disease," *IEEE Transactions on Biomedical Engineering*, vol. 62, no. 4, pp. 1132–1140, 2015.

[12] Sidong Liu, Weidong Cai, Lingfeng Wen, David Dagan Feng, et al., "Multi-Channel Neurodegenerative Pattern Analysis and Its Application in Alzheimer's Disease Characterization," *Computerized Medical Imaging and Graphics*, vol. 38, pp. 436–444, 2014.

[13] Sidong Liu, Weidong Cai, Lingfeng Wen, and Dagan Feng, "Multi-Channel Brain Atrophy Pattern Analysis in Neuroimaging Retrieval," in *IEEE International Symposium on Biomedical Imaging: From Nano to Macro (ISBI)*, pp. 206–209. 2013.

[14] Tian Xia, Dacheng Tao, Tao Mei, and Yongdong Zhang, "Multiview Spectral Embedding," *IEEE Transactions on Systems, Man, and Cybernetics, Part B: Cybernetics*, vol. 40, no. 6, pp. 1438–1446, 2010.

[15] Sidong Liu, Lelin Zhang, Weidong Cai, Yang Song, et al., "A Supervised Multiview Spectral Embedding Method for Neuroimaging Classification," in *The 20th IEEE International Conference on Image Processing (ICIP)*, pp. 601–605. 2013.

[16] Hualei Shen, Dacheng Tao, and Dianfu Ma, "Multiview Locally Linear Embedding for Effective Medical Image Retrieval," *PLoS ONE*, vol. 8, no. 12, pp. e82409, 12 2013.

[17] Sidong Liu, Siqi Liu, Sonia Pujol, Ron Kikinis, and Weidong Cai, "Propagation Graph Fusion for Multi-Modal Medical Content-based Retrieval," in *The 13th Annual International Conference on Control, Automation, Robotics and Vision (ICARCV)*, pp. 849 – 854. IEEE, 2014.

[18] Clifford R. Jack, Matt A. Bernstein, Nick C. Fox, et al., "The Alzheimer's Disease Neuroimaging Initiative (ADNI): MRI Methods," *Journal of Magnetic Resonance Imaging*, vol. 27, no. 4, pp. 685–691, 2008.

[19] John Mazziotta, Arthur Toga, Alan Evans, Peter Fox, et al., "A Probabilistic Atlas and Reference System for the Human Brain: International Consortium for Brain Mapping (ICBM)," *Philosophical Transactions of the Royal Society of London. Series B: Biological Sciences*, vol. 356, no. 1412, pp. 1293–1322, 2001.

[20] Julia A. Schnabel, Daniel Rueckert, Marcel Quist, et al., "A Generic Framework for Non-rigid Registration Based on Non-uniform Multi-level Free-Form Deformations," in *Medical Image Computing and Computer-Assisted Intervention (MICCAI)*, vol. 2208 of *LNCS*, pp. 573–581. Springer Berlin Heidelberg, 2001.

[21] Rolf A. Heckemann, Shiva Keihaninejad, Paul Aljabar, Katherine R. Gray, et al., "Automatic Morphometry in Alzheimer's Disease and Mild Cognitive Impairment," *NeuroImage*, vol. 56, no. 4, pp. 2024 – 2037, 2011.

[22] Andriy Fedorov, Reinhard Beichel, Jayashree Kalpathy-Cramer, Julien Finet, et al., "3D Slicer as an Image Computing Platform for the Quantitative Imaging Network," *Magnetic Resonance Imaging*, vol. 30, no. 9, pp. 1323 – 1341, 2012, Quantitative Imaging in Cancer.

[23] Shaoting Zhang, Ming Yang, Timothee Cour, Kai Yu, and DimitrisN. Metaxas, "Query Specific Fusion for Image Retrieval," in *European Conference on Computer Vision (ECCV)*, LNCS, pp. 660–673. Springer Berlin Heidelberg, 2012.

[24] James Bergstra and Yoshua Bengio, "Random Search for Hyper-Parameter Optimization," *Journal of Machine Learning Research*, vol. 13, pp. 281–305, 2012.